Predicting Long-Term Properties of Carbon Fiber-Reinforced Shape Memory Polymer Composites in a Low Earth Orbit Environment. (Jang et al. 2021)

Andrea Marchegiani
andrea.marchegiani@studenti.unitus.it

Master's Degree in Mechanical Engineering
Polymer and Composites for Manufacturing

16 September 2024

UNIVERSITÀ
DEGLI STUDI DELLA
TUSCIA

DIPARTIMENTO DI ECONOMIA, INGEGNERIA,
SOCIETÀ E IMPRESA

Table of contents

Shape-memory polymers Behl and Lendlein 2007

Shape-memory polymers are an emerging class of active polymers that have dual-shape capability.

They can actively change from a temporary shape A to a permanent shape B.

Such applications can be found in:

- Smart fabrics;
- Heat shrinkable tubes;
- Films for packaging;
- Self deployable sun sails;
- Implants for surgery;

Figure: Application of SMPs

The shape-memory effect in shape-memory polymers (SMPs) is not an inherent property but rather a result of their morphology and processing. Initially, the polymer is shaped into its permanent form B. In a process called **programming**, it is temporarily deformed into shape A. When an external stimulus is applied, the polymer reverts back to its permanent shape B.
The polymer network in an SMP consists of molecular switches and netpoints. These netpoints, which can be chemical (bond) or physical (intermolecular interactions), determine the permanent shape. Physical cross-linking occurs in block copolymers, where the domains with the highest thermal transition temperature T_{perm} act as netpoints, while those with the second highest T_{trans} act as molecular switches.

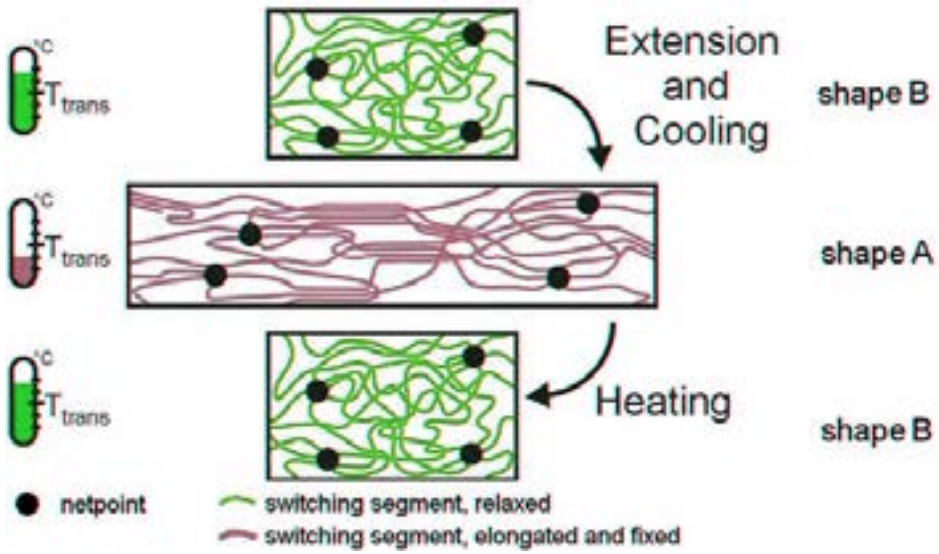

Figure: Molecular mechanism

Shape-memory properties are quantified in cyclic (N) mechanical tests for the different stimuli.

In these cyclic tests are tested:

- The **strain fixity rate** R_f, that quantifies the ability to fix a mechanical deformation ε_m, resulting in a temporary shape $\varepsilon_u(N)$;

$$R_f(N) = \frac{\varepsilon_u(N)}{\varepsilon_m}$$

- The **strain recovery rate** R_r, that quantifies the ability to restore the mechanical deformation of the permanent shape $\varepsilon_p(N)$ after application of a certain deformation ε_m;

$$R_r(N) = \frac{\varepsilon_m - \varepsilon_p(N)}{\varepsilon_m - \varepsilon_p(N-1)}$$

- T_{switch}, switching temperature in case of thermal stimulation;

A typical stress-controlled programming cycle, follows four mainly steps.

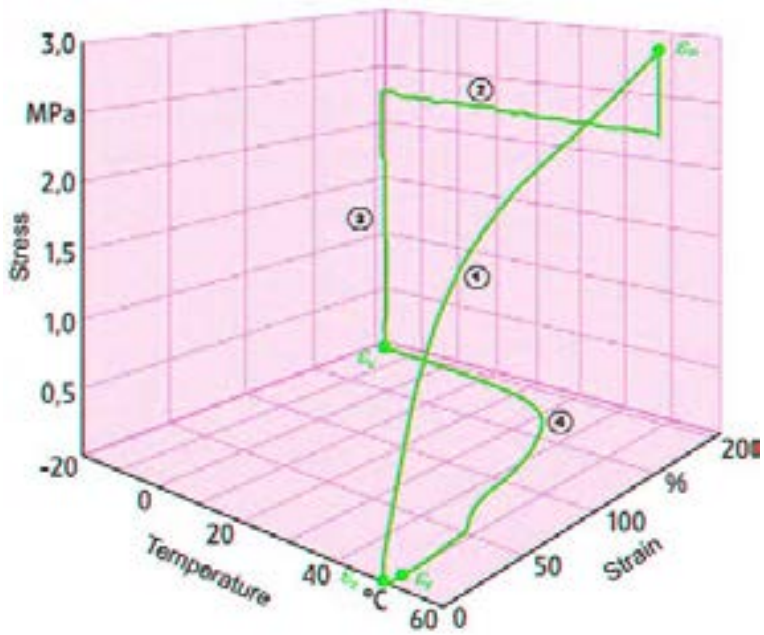

Figure: Typical stress-strain-temperature diagram

1. $T > T_{trans}$

   The sample is elongated to ε_m while the molecular switches are open.

   This strain is maintained for some time to allow relaxation of the polymer chains.

2. $T < T_{trans}$

   The molecular switchers are closing while under the action of a constant stress σ_m

3. $T < T_{trans}$

   The strain is reduced until a stress-free condition is achieved at 0 MPa.

4. $T > T_{trans}$

   While the tensile stress is held constant at 0 MPa, the molecular switches are opened again, resulting in the contraction of the test specimen and resumption of its permanent shape.

Low earth orbit (LEO) environment

Low Earth Orbit (LEO) is a popular location for satellite launches, but it presents several challenges for spacecraft due to its harsh environment. This environment includes atomic oxygen, ultraviolet radiation, ionizing radiation, ultra-high vacuum, thermal cycles, micrometeoroids, and orbital debris, all of which can degrade materials and electronic components.

- Variable altitudes: 200-1000 km
- Ultra-high Vacuum: 5×10^{-5} Torr
- Thermal cycling: $\pm 150\,^{\circ}\mathrm{C}$
- UV radiation: 100 - 200 nm
- Atomic Oxygen (AO) flux: 10^{13} - 10^{15} $\frac{\text{atoms}}{\text{cm}^2\,\text{s}}$
- Orbital Debris at velocities of 15 $\frac{\text{km}}{\text{s}}$
- Satellite velocity 8 $\frac{\text{km}}{\text{s}}$

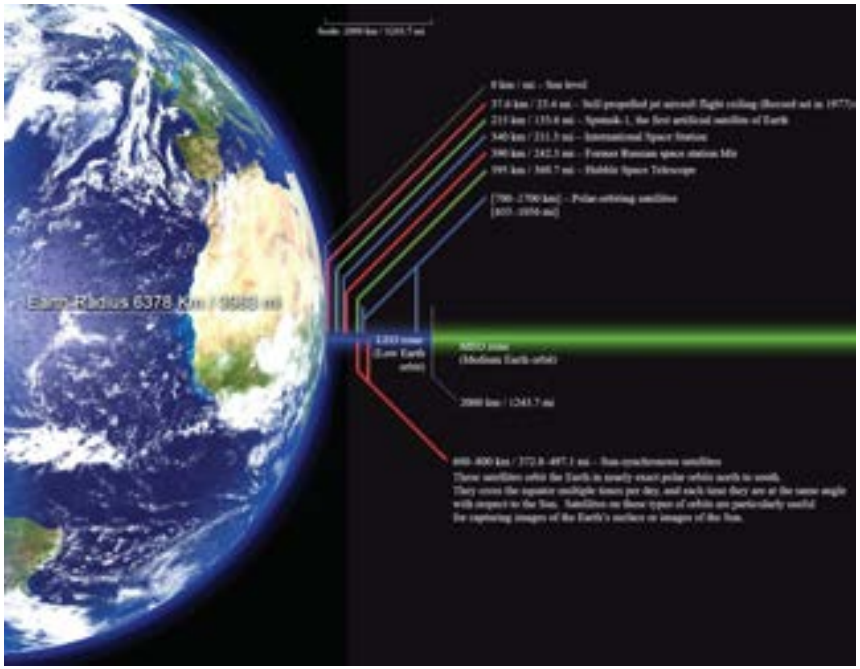

Figure: Orbital altitudes Courtesy of Mark Mercer

Aim of the research

Carbon fiber-reinforced shape memory polymer composites (CF-SMPCs) have been researched as a potential next-generation material for aerospace application, due to their lightweight and self-deployable properties.

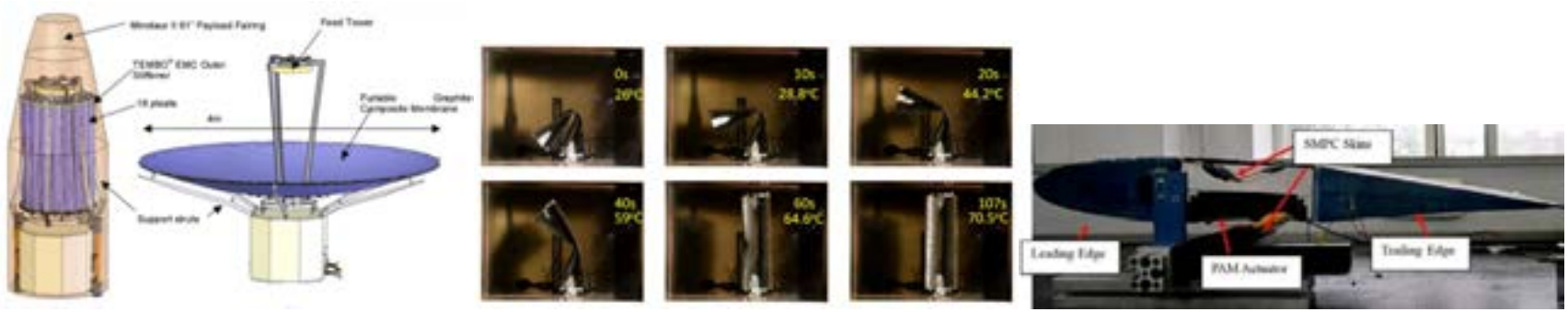

Figure: Aerospace application of SMPCs

In this study was investigated the storage modulus (G) under simulation of a low Earth orbit (LEO) environment involving three harsh conditions: high vacuum, atomic oxygen flux (AO) and ultraviolet (UV) light exposure.

The effects of the three harsh conditions on the properties of CF-SMPCs were characterized individually, using accelerated tests conducted at various temperatures in a space environment chamber, and then, combined using the time–temperature superposition principle (TTSP).

Introduction

In the LEO environment:

- High vacuum can lead to outgassing of polymer matrix
- UV radiation can break the molecular bonds of the polymer
- AO flux causes the surface erosion degrading the mechanical properties
- The temperature range can lead to microcracks due to the difference in the thermal expansion coefficient of the fiber and the matrix

So, accelerated test are commonly used to predict long-term properties and durability. In short-duration experiments, accelerated tests are conducted under conditions that are harsher than those of the target environment to project long-term performance.
The TTSP provides the means to measure long-term behavior at a specific temperature, by carrying out experiments at a higher temperature and within a shorter time.

Materials and Methods

Sample preparation

- **Thermosetting continuous phase**
  Epofix (Bisphenol A, BPA) + Jeffamine D-230 as diamine curing agent.
- **Fiber reinforced phase**
  Four layers of TI-3101 woven carbon fabric.
- **Manufacturing process**
  Vacuum-assisted resin transfer molding.
  - First curing at 110 °C for 3 h
  - Second curing at 80 °C for 2 h

Environmental Chamber

- High vacuum pump
- Cryogenic pump
- Deuterium lamps
- Plasma source with an ion accelerator

Figure: Space environmental chamber

Characterization

The storage modulus G and glass transition temperature T_g were measured using:

- Three-point bending machine
- Termogravimetric analysis
- Fourier transform infrared spectra
- Field-emission scanning electron microscopy

Results

Effects of AO Irradiation and Temperature on Matrix Erosion

Surface morphology of AO-irradiated CF-SMPCs was observed, and erosion of the SMP matrix was confirmed

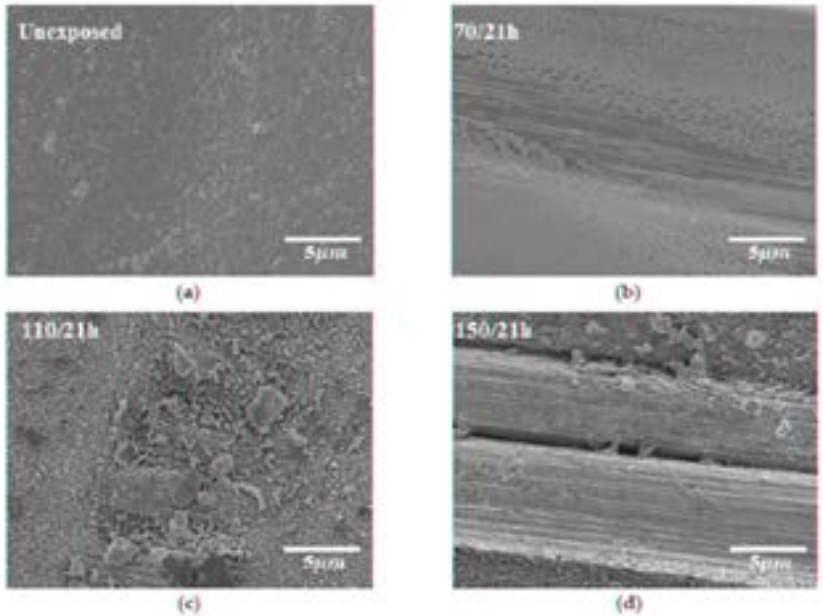

Figure: Effects of atomic oxygen (AO) exposure

In general, the interface between the fiber and matrix is weakened due to the effect of matrix erosion in an AO environment, resulting in degradation of the composite's mechanical properties.

As the exposure temperature increased, Tg increased, whereas the E decreased.

AO Exposure	T_g (°C)	**TGA Onset Temperature (°C)**
Unexposed	70	344.98
70/21 h	71	349.82
110/21 h	73.5	349.17
150/21 h	84	361.67

The erosion of the matrix by atomic oxygen (AO) can increase the weight fraction of the reinforcing material, leading to a higher glass transition temperature (Tg). However, the interaction between the polymer chains and the fibers can influence the chain kinetics in the area surrounding the fibers.

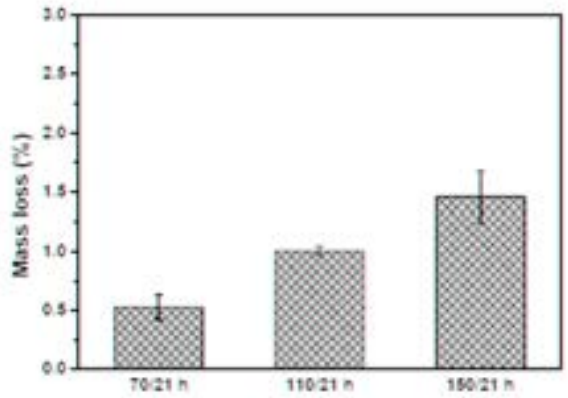

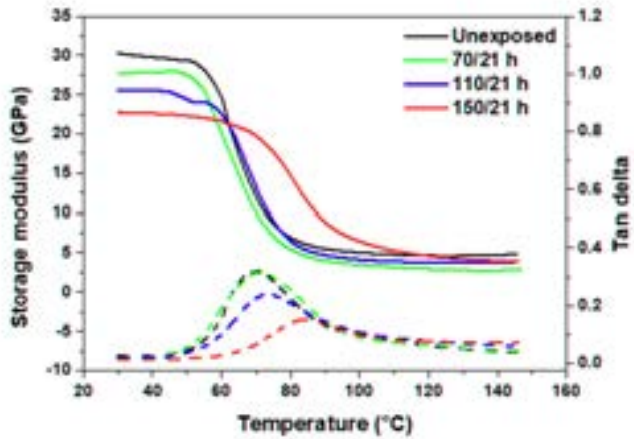

FTIR spectroscopy let us notice three characteristic peaks:

1. $1250\,\mathrm{cm}^{-1}$ is related to the Ethylene oxide
2. $1509\,\mathrm{cm}^{-1}$ is associated with N-H bond
3. $1610\,\mathrm{cm}^{-1}$ corresponds to the C-N bond

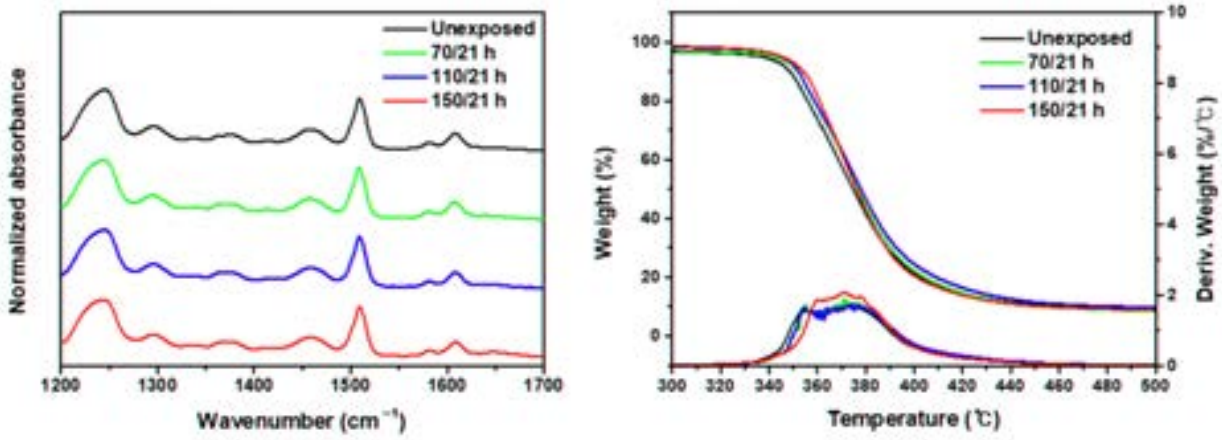

TGA curves permit us to notice the temperature of degradation.
The onset temperature before was smaller than the one obtained after AO flux at $150\,^{\circ}\mathrm{C}$, this suggest the possibility of post-curing by AO: high energy breaks the molecular chains inside the polymer, and the radicals generated create crosslinks.

Quantitative Analysis of the AO Effect on Long-Term Properties

Given that the AO effect accelerates with increasing exposure temperature, the TTSP was applied to evaluate the long-term properties due to this effect.

Using the Arrhenius equation (eq. 1, 2), shifting values were calculated. Subsequently, a validation test was conducted using a new set of temperatures: 150 °C/21 h, 139 °C/50 h, 129 °C/100 h, 124 °C/150 h, and 120 °C/200 h, with different fiber orientations.

The results obtained were highly valid, demonstrating that the prediction model based on the acceleration test can be applied to polymer composites regardless of fiber orientation, as there were no significant differences among the five validation sets.

Acceleration Effects and Long-Term Properties under LEO Environment
To obtain more accurate and representative results for the LEO environment, we will conduct accelerated tests that combine AO exposure with UV irradiation.

A significant trend observed is that, while applying harsher conditions increases T_g as expected, the storage modulus now shows an upward trend, contrary to the behavior observed with AO flux alone.
This was because both UV and AO exposure resulted in the formation of radicals via the breaking of bonds in the polymer matrix, thereby causing post-curing to occur competitively.

Both UV and AO promoted post-curing, which resulted in an increase in the storage modulus.

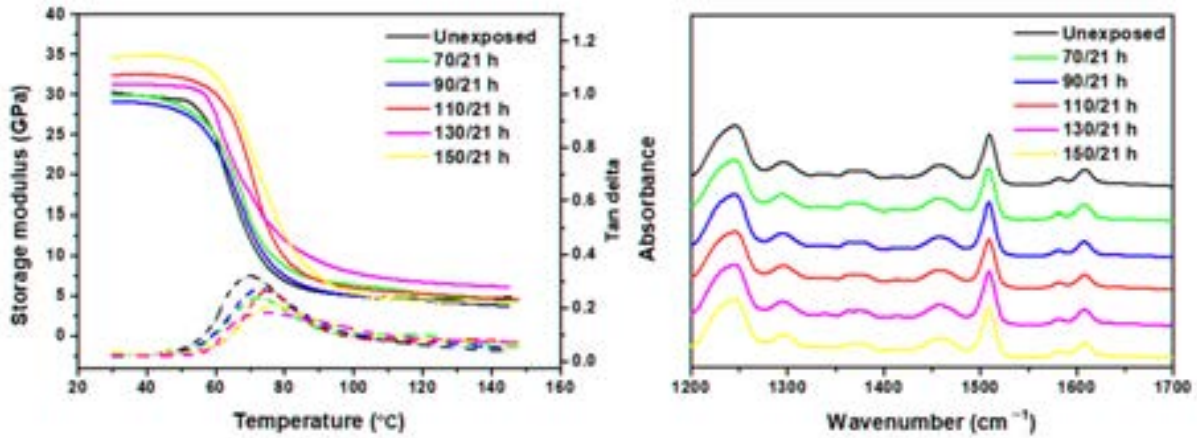
Storage modulus (GPa)
Tan delta
Temperature (°C)
Unexposed
70/21 h
90/21 h
110/21 h
130/21 h
150/21 h
Absorbance
Wavenumber (cm⁻¹)

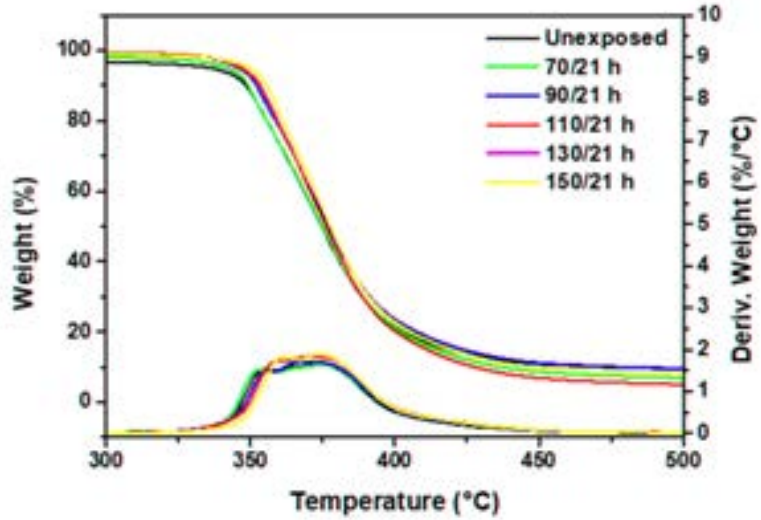
Weight (%)
Deriv. Weight (%/°C)
Temperature (°C)
Unexposed
70/21 h
90/21 h
110/21 h
130/21 h
150/21 h

In order to provide the right shifting coefficient now we have to set:

$$\log a_{LEO} = \alpha \log a_{UV} + \beta \log a_{AO}$$

And the choose of the right Arrhenius equation (eq. 3) we can obtain the master curve.

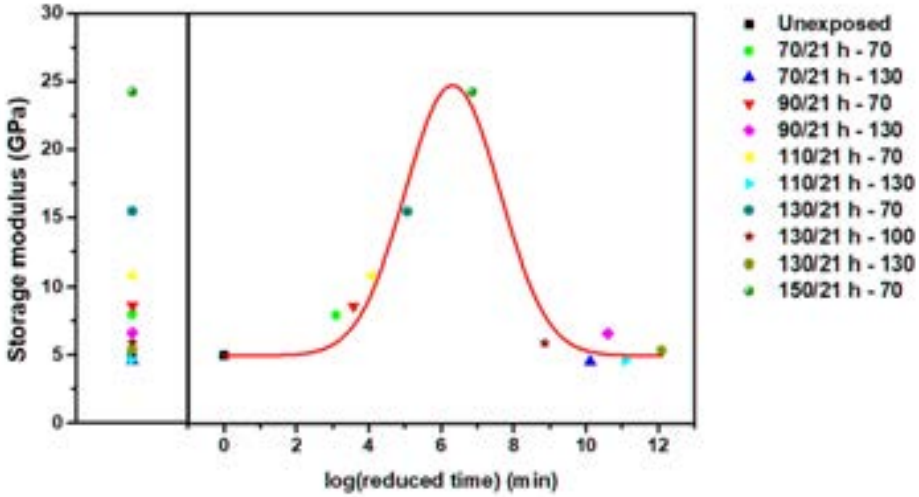

After exposure, post-curing was dominant in the early part; however, in the second half of the curve, time-relaxation aging and AO-induced degradation were prominent.

The master curve displays a sort of viscoelastic behavior with a distinct peak attributed to UV- and AO-induced oxidative post-curing. The enhancement in storage modulus at the peak correlates with increased crosslink density, whereas the subsequent decrease may be associated with post-curing saturation or degradation.

Different exposure regimes influence the kinetics of post-curing, highlighting the complex interplay between environmental factors and the material's reactivity.

Shape Memory Properties under LEO Environment

There was no significant change in shape memory performance before and after exposure to the AO and LEO environments. The fixity and recovery ratios were about 89% and 97%, respectively, indicating good shape memory behavior.

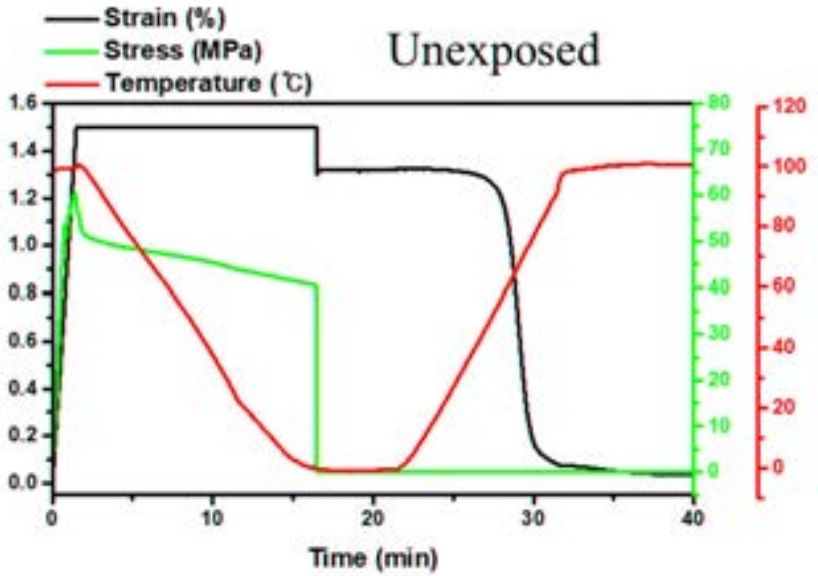

(c)

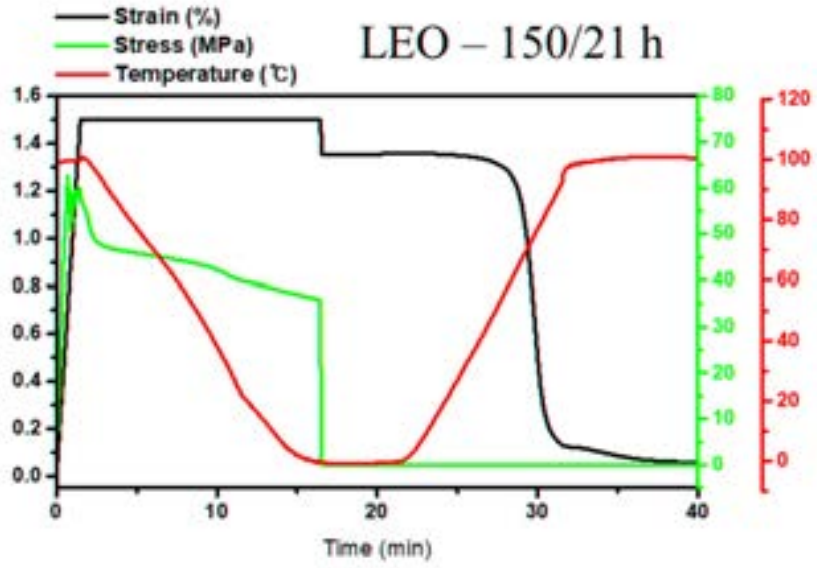

(d)

The shape memory performance of epoxy-based thermosetting SMPCs was determined based on the net points of the crosslinking structure and the flexible switching segments. In this epoxy-based material, the crosslink points act as a net point like an anchor, while the main chain of epoxy acts as a flexible switching segment. As such, the number of crosslink can determine the shape memory performance.

In AO and LEO spaces, post-curing of CF-SMPCs progressed and crosslinking increased; however, there was no further change in shape memory performance, as crosslinking had already occurred sufficiently.

Conclusions

In order to understand the underlying mechanisms governing the degradation of CF-SMPCs in a LEO environment, it is imperative to delve into their performance characteristics:

1. **AO environment**
   Surface erosion leading to smaller G and higher T_g due to the rise of weight fraction of the reinforcing material.
2. **LEO environment**
   Post curing process leading to higher G and T_g due to the formation of more cross-linked radicals.

Thank you for your attention

References


Behl, Marc and Andreas Lendlein (2007). "Shape-memory polymers". In: *Materials Today* 10.4, pp. 20–28. ISSN: 1369-7021. DOI: https://doi.org/10.1016/S1369-7021(07)70047-0. URL: https://www.sciencedirect.com/science/article/pii/S1369702107700470.


Jang, Joon-Hyeok et al. (2021). "Accelerated Testing Method for Predicting Long-Term Properties of Carbon Fiber-Reinforced Shape Memory Polymer Composites in a Low Earth Orbit Environment". In: *Polymers* 13.10. ISSN: 2073-4360. DOI: 10.3390/polym13101628. URL: https://www.mdpi.com/2073-4360/13/10/1628.

Appendix A - ASTM-E2089

The AO flux in this environment was verified based on the ASTM-E2089 standard, in which the AO flux is predicted based on the mass change of a reference material: Kapton.

$$f = \frac{\Delta M}{A \rho E t}$$

where f is the effective AO flux, ΔM is the mass change of the reference materials, A is the exposed area, ρ is the density, E is the erosion yield, and t is the exposure duration. The AO flux was calculated based on the mass loss measured over a 21-h exposure period.

Appendix B - TTSP Arrhenus formulations

$$G(t, T^{AO}) = G^{ref}\left(\frac{t}{a_{AO}(T)}, T^{AO,ref}\right) \tag{1}$$

where G^{ref} refers to the storage modulus of CF-SMPCs exposed at the reference temperature, $T^{AO,ref}$ is the reference exposure temperature (70 °C), $a_{AO}(T)$ is the shift factor at the exposure temperature, and G is the predicted storage modulus of CF-SMPCs at the exposure temperature.

$$\log a_{AO}(T) = \frac{\Delta H_{T,AO}}{2.303R}\left(\frac{1}{T^{AO}} - \frac{1}{T^{AO,ref}}\right) \tag{2}$$

Where $\Delta H_{T,AO}$ is the activation energy that for the AO process was 84.16 KJ/mol.

$$G(t, T, T^{LEO}) = G^{ref}\left(\frac{t}{a_T(T)a_{LEO}(T)}, T^{ref}, T^{LEO,ref}\right) \tag{3}$$